CORE
Metadata, citation and similar papers at core.ac.uk
Provided by NERC Open Research Archive

<articletype>Original

<title>Geomorphology of the western slope of Hatton Bank (Rockall Plateau, NE Atlantic Ocean) revealed by multibeam bathymetry and high-resolution seismic data: control by bottom current regime>

<author>M. Sayago-Gil, D. Long, K. Hitchen, V. Díaz-del-Río, L.M. Fernández-Salas, P. Durán-Muñoz

M. Sayago-Gil (corresponding author) (e-mail: miriam.sayago@ma.ieo.es, Tel.: +34-952-478148, Fax: +34-952-463808), V. Díaz-del-Río, L.M. Fernández-Salas
Instituto Español de Oceanografía, Centro Oceanográfico de Málaga, Puerto Pesquero, s/n, Apdo. 285, 29640 Fuengirola, Spain
D. Long, K. Hitchen
British Geological Survey, West Mains Road, Edinburgh EH9 3LA, UK
P. Durán-Muñoz
Instituto Español de Oceanografía, Centro Oceanográfico de Vigo, Cabo Estay-Canido, Apdo. 1552, 36200 Vigo, Spain

Received: 20 March 2009 Accepted: X XXXX 2009

Abstract

A geomorphologic study, using multibeam data as well as high- (airgun and sparker) and very high-resolution (topas) seismic profiles from the western slope of the Hatton Bank (NE Atlantic), in 600 to 2000 m water depth, has identified a range of geomorphologic features in an oceanographic setting. Two principal sea-bed domains have been recognised: (1) a non-depositional area (corresponding to the top of the bank) and (2) a depositional area in which the Hatton Drift has developed. Five morphological areas have been identified associated to both domains: in (1) outcrop and ridges areas and in (2) smooth surface, slides and bedforms areas controlled mainly by bottom currents interacting with the topography of the bank that describing the boundaries between two water masses (probably the Labrador Sea Water and the upper limit of the Lower Deep Water). Individual features as: contourite channels (moats, furrows and scours), wave fields, contourite-packages boundary, ponded deposits, scarps,

gullies, ridges, depressions and slides, were identified on these areas. These morphologies can be due to past events and does not necessarily reflect the present-day current conditions.

<heading1>Introduction

The effect of the bottom currents in shaping the sea bed over both depositional (drift) and erosional characteristics is well known (Hollister and Heezen 1972; McCave and Tucholke 1986; Masson et al. 2004). The sea floor is sculpted into a wide variety of bedforms (flow can erode, mould, transport and redistribute sediments) that gain an insight into bottom currents features (Stow et al. 2008). Recent studies by Kuijpers et al. (2002); Masson et al. (2004) and MacLachlan et al. (2008) have used bedforms and related erosional features to map the distribution of bottom currents in NE Atlantic Ocean. As recently reviewed by MacLachlan et al. (2008) in Hatton Bank margin, the interaction between bottom currents and slope configuration, control the morphology of the deposits.

In this paper we present a geomorphologic study of the western slope of Hatton Bank using multibeam data and high-resolution seismic profiles in order to identify possible depositional, erosional and gravitational features. We then attempt to interpret these in terms of existing knowledge of the regional bottom current regime.

<heading1>Physical setting

<heading2>Physiography

The Rockall Plateau comprises the shallow-water banks of Rockall Bank, Hatton Bank (object of this work) and George Bligh Bank. Hatton Bank is separated from Rockall Bank by the Hatton-Rockall Basin (Roberts et al. 1970; Fig. 1) and has a sinuous bathymetric planform. South of 59ºN, it is aligned approximately SW–NE and further north the alignment is more W–E (Hitchen 2004). The study area is located between 600 and 2,000 m water depth on the western upper and middle slope of Hatton Bank (Fig. 1) which is a slope remote from any major terrigenous sediment supply; at present, it lies over 360 km from the closest onshore sediment source (MacLachlan et al. 2008). The area is dominated by contourite drifts that are the primary deposits of bottom currents (Weaver et al. 2000). Contourites are deep-sea sediments that accumulate under the influence of strong thermohaline bottom currents.

<heading2>Oceanography

In the mid-latitude NE Atlantic Ocean, Van Aken (2000) categorised the Northeast Atlantic Deep Water in terms of four local source water types: the Iceland-Scotland Overflow Water,

Lower Deep Water, Labrador Sea Water and Mediterranean Sea Water. The western slope of Hatton Bank is influenced by a branch of the Labrador Sea Water which meets with the Iceland-Scotland Overflow Water, forming the Deep Northern Boundary Current (McCartney 1992; Fig. 1), and possibly by the Lower Deep Water (Bianchi and McCave 2000) which travels toward NE from the southern part of Hatton Bank until 58–59ºN before turning westwards into the Iceland Basin circulating anticlockwise (Van Aken 1995). Hunter et al. (2007) propose that the upper and lower limits of the Labrador Sea Water are at about 700 and 1,500 m water depth respectively in the Iceland and Irminger Basins, consistent with the overall water depth of 1,000 m described by McCartney (1992). In addition, Due et al. (2006) reported northward currents in the permanent thermocline above a water depth of approx. 1,500 m. McCave et al. (1980) also documented a strong NE-flowing bottom current along the foot of Hatton Bank, comprising North Atlantic Deep Water with some admixture of Antarctic Bottom Water. Measured current velocities in this area reach a maximum of 23 cm s^{-1} (Stow and Holbrook 1984).

<heading2>Geology

The Rockall Plateau is a broad, topographically elevated region in the NE Atlantic Ocean, underlain by continental crust which, before the opening of the North Atlantic Ocean in the Mesozoic to early Cenozoic (Stoker et al. 1998), was juxtaposed between Greenland and Europe. The present-day configuration of the Rockall Plateau is the result of a complex geological evolution involving continental plate movements, tectonics, massive volcanism, and differential subsidence and inversion (Hitchen 2004). The Rockall Plateau comprises a volcanic continental margin with the continental-ocean transition located beneath the lower western slope of Hatton Bank (Kimbell et al. 2005; Smith et al. 2005). The south part of Hatton Bank, (at least part of the underlying geological structure) comprises an inverted Cretaceous (and older) to Paleocene basin (McInroy and Hitchen 2008). Further north the structure comprises a large anticline with minor thrusts climbing up its southern limb (Hitchen 2004). Widespread early Palaeogene flood basalts sub-crop (and occasionally crop out) over most of the Rockall Plateau. Although not definitely proven, the tectonism within the Hatton Bank appears to become more intense, and younger, northwards (Hitchen 2004). Although commonly described as ‘passive’, the NE Atlantic Margin adjacent to the British Isles, of which the Rockall Plateau is a component, has undergone significant tectonic activity throughout the Cenozoic. This includes basin margin tilting, differential subsidence and the

formation of large scale structural domes and ridges due to episodic compression (Stoker et al 2005, Johnson et al. 2005, Tuitt 2009).

The *Hatton Drift* (Ruddiman 1972; Fig. 1) was classified by McCave and Tucholke (1986) as a plastered-contourite drift which lies at the foot of the NW side of the Rockall Plateau and is composed mainly of mud (McCave et al. 1980). Sediment transport along the Hatton Drift to the northeast is both by suspended transport of fines in locally generated nepheloid layers and by bedload transport of cohesionless sand (McCave et al. 1980). Linear erosive features were described by Hernández-Molina et al. (2008) including large contourite channels and smaller elongate furrows, as well as channels related to slope drifts (contourite moats). Sediment drifts in the NE Atlantic have maintained their basic characteristics at least since the mid-Pleistocene (Huizhong and McCave 1990).

<heading1>Materials and methods

<heading2>Multibeam data

Within the framework of the *Ecovul-Arpa* project (http://www.ieo.es/proyectos/pesquerias/ecovularpa.htm); Kongsberg-Simrad EM300 multibeam echosounder data were collected between 2005 and 2007, providing 100% coverage of the whole study area (18,760 km^2) from 600 to 2,000 m water depth (Fig. 2). The data were processed with the CARAIBES software© (http://www.ifremer.fr/fleet/equipements_sc/logiciels_embarques/caraibes/index.html), and a 50×50 m resolution grid produced. In addition, backscatter mosaic was extracted from the multibeam data. Morphologic analysis was done using ArcGIS Desktop.

<heading2>Seismic data

High-resolution airgun and sparker seismic data were acquired in 1992, 1998 and 2002 along 2,840 km with line spacing varying between 5 and 20 km (Fig. 2). The airgun system consisted of an array of four 40-$inch^3$ Bolt guns connected to a 30-m Geomechanique hydrophone cable. All channels were summed for optimum output. Sparker data were collected at up to 3-kJ maximum power via a 10-m Teledyne hydrophone cable. In both cases, the power and firing rate varied according to water depth. All data were stored onto a CODA DA200 recording system and navigation was by DGPS.

From 2005 to 2007, a network of approx. 1,120 km of very high-resolution seismic profiles was collected with a parametric Topas PS 018 echosounder (Fig. 2b), at 16–20 kHz. The data were processed by means of Kingdom Suite software (http://www.seismicmicro.com/).

<heading1>Results

Figure 3 presents a general overview of dominant seabed morphology and the slope gradients recorded in the study area. The study area can be subdivided in two main domains (Fig. 3a): (1) an area where little or no deposition occurs (outcrop) and (2) a depositional area (drift). (1) The outcrop shows at the most only thin (<20 ms) sediment deposits, mainly shallower than 1,100 m water depth (Fig. 3a) and it is characterized by an uneven surface. Seabed gradients (Fig. 3b) reaching 40º occur locally and high backscatter values (>-20 dB) are typical. A special morphological area, named "ridges area" (Fig. 3c), can be described associated to the outcrop forming a series of parallel barriers extended up to 1,600 m water depth.
(2) Downslope, a surface recognised as the top of the Hatton Drift (Fig. 3a) has been identified. It follows the general trend of the slope of the bank and overall has gradients of 0–3º (Fig. 3b), reaching 30° in places (e.g. moats). It exhibits moderate–low backscatter values (generally <-20 dB). Based on the seismic data, this surface belongs to a deposit characterized by variable sediment thickness (>400 ms downslope), generally increasing basinward and onlapping upslope as a wedge with well-stratified layers (Fig. 2b). In places, this deposit can be seen covering the outcrop. There are three main morphological areas associated to the drift: smooth surface area, bedforms area and slides (Fig. 3c). The sediment drift exhibits differences in seabed morphology at water depths shallower and deeper than 1,400–1,500 m. Upslope, the sea bed has smooth relief whereas downslope the uneven surface contains furrows, scours and slides. The "smooth surface" (Fig. 3c) is located in the southern part (Fig. 3a) of the study area between ~1,100 and ~1,400 water depths (except attached to the "ridges area" where the "smooth surface" is reduced). In the "bedforms area" (Fig. 3c) the drift shows an irregular surface and it is located contouring the outcrop in the northern part of the study area with a minimum of ~1,100 m water depth, whereas in the southern part the "bedforms area" is deeper than ~1400 m water depths. "Slides" (Fig. 3c) are located in the southern part and the headwalls of the slides are at ~1400 m water depths.

Individual features– contourite channels (moats, furrows and scours), wave fields, contourite-packages boundary, ponded deposits, scarps, gullies, ridges, depressions and slides– are described in more detail (Fig. 4-7):

<heading2>Contourite channels

We distinguished three types of contourite channels, occurring mostly in groups.

1. *Moats* (Fig. 4a) typically occur at the boundary between the areas of outcrop and drift formation, at 1,000–1,300 m water depth and are characterised by a main axis parallel to the bathymetric contours. Mean moat length is 23 km (range of 14–38 km), and mean width 1.3 km (maximum of 3.5 km). In cross section, the upslope bedrock surface of the moat is steeper than the downslope drift surface, below which the internal reflectors of the drift illustrate decreased sedimentation into the moat. The gradient recorded on such drift flanks has a mean value of 2º, but reaches maximum values of 30º at some locations. In the northern part of the study area, two wave fields have been identified associated with moats drift-flanks (c.f. below) and the crest of waves are oblique to the moats axis.

2. *Furrows* (Fig. 4b) trend parallel to the bathymetric contours and possess different plan geometries each other. On the whole, they are characterised by a single axis, (although some show an axis bifurcation). The furrows usually have flat bottoms (although occasionally small ridges are observed inside) and steep sedimentary sides (Fig. 4b). The furrows are located between 1400 and 1800 m water depth and have a mean length of 9 km (range of 3-34 km). The mean gradient of the furrow walls varies: those on the northern slope of Hatton Bank (axis with W–E trend) have typical gradients of 6–7º on the northern wall and 16–17º on the southern wall (upslope); and furrows further south, where the slope of the bank faces west, have shallower gradients, typically 2–3º on the western wall and 5–6º on the eastern wall. On seismic data, furrows exhibit a complex history of excavation, erosion on the flanks and partial infilling by drift sequences.

3. *Scours* (Fig. 4c) can be detected on the multibeam bathymetry data as U-shaped scars at only shallow depths (5–15 m) and vary in length between 1 and 29 km. Scours can not be detected clearly on seismic data owing to the fact that the scale of the profiles and in places, can be observed on the backscatter mosaic with higher values (~22 dB) than the surrounding areas. They are orientated parallel to the main trend of the bathymetric contours and are adjacent to others morphologies such as furrows.

<heading2>Wave fields

Two wave fields occur in the north of the study area, on the flanks of moats.

1. The western wave field (Fig. 5a) covers an area of 10.2 km^2 (6 by 1.7 km), between 1,180 and 1,270 m water depth. Mean wave heights are 15–20 m, mean wavelength 0.9 km, and the waves are symmetric.

2. The eastern wave field covers an area of 18.3 km^2 (7.8 by 2.7 km) in water depths between 1,390 and 1,500 m. The waves are symmetric, with amplitude of 5–7 m and wavelengths varying between 0.4 and 1.2 km. Crest orientation changes from overall SE–NW on the flank to E–W towards the axis of the moat.

<heading2> Contourite-packages boundary

The multibeam imagery provides evidence of a concave boundary in the form of a marked change in the overall slope gradient of the Hatton Bank at the limit between two contourite packages (Fig. 5b), occurring between 1,000 and 1,300 m water depth and has a length of 40 km. The gradient is 2–3º upslope and 0.3–1º downslope. On seismic data, the boundary marks the upslope limit of an accreting drift wedging out against a lower drift deposit.

<heading2>Ponded deposits

Sediments which fill irregular hollows in the bedrock surface (or located in surrounding areas) are here termed ponded deposits (Fig. 5c). On multibeam bathymetry theses deposits appear as flat surfaces between crests of outcropping bedrock. On seismic profiles, they can be recognised by well-stratified layers onlapping against the outcrops. In places surrounding outcrops, the sediments are forming wedge-shaped deposits with a downslope progradational internal structure. Sediment thickness (up to 50 ms) and area (40 km^2) vary depending on the surrounding outcrop geometry. Ponded deposits show low backscatter, in contrast to the adjacent outcrop.

<heading2>Scarps

Scarps are shown as abrupt gradient changes which divide two areas with different level and softer gradient, and the majority of which face downslope (Fig. 6a). The strike of the scarps usually parallels that of the regional slope. The scarps are located in both the outcrop and sediment drift areas. The gradients vary between 3 and 10º, although they can reach 20–30º locally. The height is up to 55 m and generally, the areas around the scarps show a high backscatter (~20dB).

<heading2>Gullies

In the south of the study area two gullies are recognized between 1100 and 1300 m water depth showing sinuous shapes, in plan view, crossing the main trend of the bathymetric

contours with an overall WSW–ENE orientation (Fig. 6b). Usually the southern side of the gullies is steeper than the north side with gradients of 7–8°, reaching 15° at some locations. The side-wall scarp varies in height but reaches a maximum value of 70 m in the easternmost part of one of the gullies. Both gullies are approximately 4 km in length although the southern one may previously have been up to 8 km (Fig. 6b). There is strong evidence for infilling of other gullies (or lateral migration of the same gully) in the immediate vicinity leaving only a shallow present-day depression of up to 10 m. This is corroborated by the seismic profile which illustrates a deep erosive gully and now partially infilled by sediments prograding downslope leaving a highly asymmetric present-day profile (Fig. 6b).

<heading2>Ridges

In the outcrop area there is a series of parallel and elongated ridges 5 km apart above 1600 m water depth. Ridges are long narrow raised land formations with sloping sides which show common segmentation (Fig. 6c) with sections of 2–7 km length, with four main orientations: N90ºE, N78ºE, N67ºE and N53ºW. The heights of the ridges vary between 5 and 45 m and generally have steeper gradients downslope (up to 17º). There maybe a thin veneer of sediment on these features. Ridges are associated to ponded-deposits explain above (Fig. 5c). Superimposed on the ridges are conical mounds (Fig. 6c); some of them symmetrically shaped single features whereas others are asymmetrically-shaped features formed by coalescing former individual mounds. These mounds stand 10 to 25 m above the ridges and are a few hundred metres in width.

<heading2>Depressions

The depressions appear on the multibeam bathymetry as near-circular with areas of 0.2–0.9 km^2, variations in depth between 20 and 30 m (Fig. 6d) and have steeper upslope sides (7–10º) compared to the downslope sides (2–4º). Some of them show a backscatter change between the bottom of the depressions (up to -17dB) and the surrounding areas (~ -35db).

<heading2>Slides

The data have revealed two slides.

1. The *Talismán Slide* (Sayago-Gil et al. 2009) (Fig. 7), at the southern western edge of the study area (Fig. 3c), covers a minimum of 194 km^2 and extends at least 15 km downslope. It is a very conspicuous feature with only the thinnest post-slide veneer of sediments. The slide

is orientated E-W from its headwall scar at 1358 m water depth and to, at least, 1900 m water depth. The 7.7-km headwall scar shows a SW–NE trend with an irregular zigzag form. The scarp varies in height between 50 and 76 m and has a slope angle of 34º. The northern sidewall has a linear NW-SE trend with a scarp height of up to 100 m. The southern sidewall has an irregular form, comparable to the headwall, with a scarp height of 50 m decreasing downslope to 30 m and with slope angles of 25–30º. The remnant surface of the slide mass shows discontinuous morphologies (Fig. 7). There are depressions in the surface and upstanding blocks (with a relief up to 20 m), both of which have a step-like appearance. Seismic data show the remnant slide mass is 10–20 m thick above the slide plane. The slide plane cuts into a sequence of contourite deposits.

2. About 160 km north of the Talismán Slide (Fig. 3c), a partially buried slide, informally named the *Granadero Slide* (Sayago-Gil et al. 2009), has been reported by MacLachlan et al. (2008) using independent dataset. Here, we expand the earlier findings with new information forming part of the results of the present study. The multibeam data show it covers an area of 230 km^2 and extends at least 11 km downslope in an E–W orientation. Its headwall scarp is at 1385 m water depth and the slide extends to at least 1980 m water depth. The 18 km headwall scar has a NE–SW trend. The maximum height of the headwall scar is 68 m but the sidewalls may locally reach 120 m. The slope angles of the sidewalls are on mean 6° but may locally reach 24° on the northern sidewall. The slide mass shows a slope angle <3°. The seabed within the slide area exhibits a smooth relief with some gentle waves mainly parallel to the headwall. However, a single mounded deposit, attached to the southern sidewall, is more than 60 m high. These sediments are contourite deposits accumulated in the lee of sidewall since the slide event.

A new morphological sketch of the part studied of Hatton Bank is presented in figure 8, showing the bedform details of the two main domains describe in this work (outcrop and drift) in the northern and southern parts of the bank. The outcrop area is characterized by an uneven surface with crest and scarps and the ridges area can be seen with ponded deposits associated. Three main morphological areas have been associated to the drift: smooth surface area, bedforms area and slides. The smooth surface is nearly a flat surface located in the southern part of the bank. Bedforms area are describe as a surface with different morphologies as furrows, scours and scarps located in the northern part as well as in the southern part of the bank. Slides can be seen in the southern part close to bedforms areas.

<heading1>Discussion

In a general overview, the study area can be divided in two main domains: (1) outcrop and (2) drift, where the limit is about 1,100 m water depth.

(1) Outcrop is characterized by an irregular surface (due to tectonic activity and erosion) with crests and escarpments trending predominantly W-E and lag deposits of coarse sands and pebbles-boulders that give the high backscatter with only small areas of true outcrop (C. Jacobs, Pers. Comm.). Smith et al. (2005) described this area as a bedrock surface composed by flood basalts which were dated by McInroy et al. (2006) as late Palaeocene although in some areas may be Palaeogene and younger rocks. In places flood basalts are absent and the underlying Mesozoic sediments are imaged on seismic data (Hitchen 2004). Within the outcrop area many ridges (constructional basalt scarps originated probably by faults in depth) may owe their origin to compressional tectonics (Tuitt 2009) and conical mounds (individual or clustered) superimposed (10-25 m high) have been observed in this study. The mounds of Hatton Bank bear a strong resemblance, albeit smaller in size, to features reported in the Porcupine Seabight (Bailey et al. 2003) and at the southern end of the Rockall Bank (Van Weering et al. 2003) and proven to be bioclastic accumulations sustained by the growth of cold water corals. Small mounds on the crest of Hatton Bank are principally comprised of *Lophelia pertusa* (Roberts et al. 2008). The bare rock surface provided by the ridges has been opportunistically exploited by the corals leading to the development of the mounds. Ridges have been linked with cold-water corals in this area as a suitable substratum to their growth. Many samples of cold-water corals have been collected on the ridges under the Ecovul-Arpa project and they demonstrate the presence of alive and dead corals. The mounds bulk probably comprises dead cold-water corals that provide the platform for further growth of corals. Ridges act as barriers forming ponded deposits infilling and surrounding the uneven surface. These deposits result from the alongslope and downslope movement of sediment which becomes trapped in the irregular surface. The deposits consist of drift sediment and coral rubble derived from the adjacent ridges and mounds. At these locations, there is the potential to preserve the oceanographic record that is absent from the rest of the outcrop area.

(2) The depositional area is dominated by the Hatton Drift which is located on the lower and middle-western slope of Hatton Bank. It is a contouritic deposit composed mainly of mud and sand (Stow and Lovell 1979) and was classified by McCave and Tucholke (1986) and Faugères et al. (1993; 1999) as a "plastered drift" which is deposited on the slope of Hatton Bank. The structural, textural and compositional attributes of the drift sediments were

described, by Stow and Holbrook (1984), in two parts: (a) those deposited prior to the onset of northern hemisphere glaciation, and (b) those deposited during the glacial-interglacial cycles. The overall morphology of the Hatton Drift and the differential rates and thickness of sediment accumulation have been influenced by bottom currents since early Eocene times (Stow and Holbrook, 1984). However, strong bottom currents at first prevented any significant deposition and it was only after mid-Miocene time that drift accumulation began. In the NE Atlantic Ocean, sediment drifts have contrasting styles which most probably reflect the interaction between a variable bottom-current regime and the complex bathymetry of the continental margin (Stoker et al. 1998). The drift can be observed in the study area with different seabed morphologies which have the main origin in the activity of bottom currents. So, there are areas with smooth surface in contrast with other areas with several kinds of bedforms due to the interaction between the bottom current contouring the topography of the bank which cause change of direction in the main current flow. The upslope walls of the furrows show usually higher gradient than downslope walls which have the origin in the interaction between the flow and the slope configuration that prompt greater erosion on upslope walls. Besides, the drift sediments moving up-and-down slope covering, in some places, the outcrop and forming ponded sediments which are trapping by the ridges.

A variety of current-induced bedform types provide further information on the bottom-current regime (e.g. Kuijpers et al. 2002). So, in the southernmost part of the bank, the sediment drift exhibits differences in seabed morphology (smooth area/ bedforms area and slides) at water depths shallower and deeper than 1,400–1,500 m which link with the lower limit to the Labrador Sea Water proposed by Hunter et al. (2007) to the Iceland Basin and the permanent thermocline described by Due et al. (2006) in the western flank of Hatton Bank. Labrador Sea Water transports sediments north-eastwards along the western slope of Hatton Bank (McCartney 1992; Due et al. 2006; MacLachlan et al. 2008). In addition, according to Bianchi and McCave (2000), the Lower Deep Water travels towards the north, from the south part of Hatton Bank until approx. 58–59ºN where it turns to the west as shown by the orientation of the furrows and other seabed features (Fig. 8). The bedform area (south 59ºN), rich in furrows and scours, may reflect an intensification of the Lower Deep Water as it turns westward owing to a topographic bulge in the slope of Hatton Bank at ~58.5ºN. However, the presence of another bedform area and another slide northward (59–59.5ºN) on the slope of Hatton Bank suggests that, at least, some of the Lower Deep Water could return to the slope of the bank north of the bulge.

The contourite-packages boundary and the moats are found along the length of Hatton Bank (Fig. 8) having been mapped in water depths ranging from 1,000 to 1300 m, which match with the fact of McCartney (1992) found some of Labrador Sea Water ~ 1,000 m water depth. In this work, we propose the upper limit of the Labrador Sea Water at 1,000-1,300 m water depth depending of the topography of the slope. The upper boundary of the Labrador Sea Water could provide a limit to the upslope migration of the drift on the western slope of Hatton Bank.

Different morphologies of the contourite deposits indicate erosion which has excavated the original furrows and truncated the reflectors within the exposed bedrock side of the moats that suggest periods of strong bottom-current erosion followed by reduced-strength currents which are responsible for the present-day infilling of the furrows and the constructive drift boundaries seen in the contourite-packages boundary and moats. Within this context it should be noted that various bedforms might result from extreme current events in the past and thus do not necessarily reflect present-day current conditions (Due et al. 2006).

In the northern part of Hatton Bank, where the bank is orientated W–E, the morphological features are typically shallower than in the southern part. This could reflect a shallowing of the oceanographic currents northwards or a change in the current regime. Likewise, MacLachlan et al. (2008) show an area in the northern part of Hatton Bank which has a wide variety of bedforms (sediment waves, furrows and moats), reflecting a complex bottom current flow from the east (occasional overflow events of Iceland-Scotland Overflow Water travelling toward south from the Faeroe Bank Channel) in contrast to the Deep Northern Boundary Current. This current activity is occurring at a shallower level than in the southernmost part of the bank with the resultant bedforms developed higher up the outer slope. Furthermore, wave fields could be originated by an opposite flow (referenced to the main direction current) occur on the drift-flank of the moats close by the area where the adjacent outcrop change the direction creating a reversed flow.

In addition, gravitational processes have been identified in the study area. Most notable are the Talismán Slide (Sayago-Gil et al.2009) clearly seen on the sea bed at the southern part of Hatton Bank (Fig. 8) and the buried slide previously noted by MacLachlan et al. (2008), both occurring within the acoustically well-layered drift sequences. Talismán Slide shows only the thinnest post-slide veneer of sediments on top which could imply a recent age, although this is highly dependent on sedimentation rate. The original dimensions of the buried slide may have

been greater but have been reduced due to partial infilling of the feature. Failures of slopes detached of the emerged land are rarely reported. A range of trigger mechanism is plausible and could include a combination of several causative factors. Changes in current regime may erode the base of the drifts thereby removing support at the base of slope (Sayago-Gil et al. 2009). Alternatively increases in sedimentation at the top of the slope may overload the upper part of the drift. Fluids, including gas, may facilitate movement in response to ground acceleration (due to earthquakes) although there is no clear evidence for shallow gas on the western side of Hatton Bank. Despite difficulties in detecting low seismic activity in Hatton Bank area from land based seismometers, earthquakes have been recorded. Two events have been detected in recent years (1998 on Hatton Bank and 1999 on Lousy Bank) to show that although this is a passive margin, it is not aseismic (Simpson and Ford 1999; Simpson et al. 2000) corroborating intra-plate seismic activity. The presence of two similar-sized slides on the outer slope of Hatton Bank suggests episodic repetition of conditions required to trigger slope failure.

The depressions on the seabed south of the Talismán Slide could be related to fluid escape (including gas) but they are larger (1 km diameter by 20 m depth) than pockmarks commonly reported for other continental margins along NE Atlantic Ocean (Paull et al. 2008; Fernández-Puga et al. 2007). However, Hammer et al. (2009), describe an upstream convergence of flow lines followed by upwelling over the pockmark which could explain the presence/maintenance of these depressions in the absence of fluid or gas seepage.

At the southern end of the study area, rock outcrops (Fig. 8) differ from the rest of the margin. This may reflect strong currents or lack of sediment supply. Higher up the bank, the seabed image shows several, partially infilled downslope gullies. These may have been cut during periods of lower sea level, at glacial maxima, when alongslope currents were reduced. The partial infill appears to be derived from the northwest, which is contrary to the present regional current regime, but which may reflect the scarcity of geophysical profiles in the area.

However, there is uncertainty concerning some of the features and further seismic profiling and ground-truthing by shallow coring as well as other oceanographic data (as for example CTDs and current-meters) are required to elucidate the sedimentary history and current regime.

<heading1>Conclusions

1. Interpretation of the multibeam and shallow seismic data has identified morphological features that can be attributed to the Labrador Sea Water and Lower Deep Water boundaries between them suggestive of a complex oceanographic regime. This limit could be located at 1,400-1,500 m water depth which would be the lower limit of the Labrador Sea Water and the upper limit of the Lower Deep Water. In addition, the upper boundary of the Labrador Sea Water could be at 1,000-1,300 m water depth and provide a limit to the upslope migration of the Hatton Drift. More oceanographic data are necessary to confirm the exact water masses affecting to the western slope of Hatton Bank.
2. The Lower Deep Water was described travelling toward north until ~58.5ºN where the bulge of the bank is. This work proposes that the Lower Deep Water could return to the slope north of the bulge ~59–59.5ºN.
3. The erosion features and present-day infilling deposits suggest periods of strong bottom-current erosion followed by reduced-strength currents. So, the present morphology of the western slope of Hatton Bank can be due to past events and does not necessarily reflect the present-day current conditions.
4. This work extends the geographical extent where cold corals have been mapped on Hatton Bank in the ridges area until ~ 1,500 m water depth.

Acknowledgements

This work was supported by the Ecovul/Arpa project, Instituto Español de Oceanografía IEO and Secretaría General del Mar, Spain. Thanks are due to IEO for multibeam bathymetry and Topas seismic profiles and to the British Geological Survey for airgun and sparker seismic profiles. DL and KH publish with the permission of the Executive Director of the British Geological Survey (NERC). We are grateful for the comments and suggestions of C.L. Jacobs, G.M. Elliot and M.T. Delafontaine who reviewed the manuscript.

References

Bailey W, Shannon PM, Walsh JJ, Unnithan V (2003) The spatial distribution of faults and deep sea carbonate mounds in the Porcupine Basin, offshore Ireland. Mar Petrol Geol 20:509–522

Bianchi GG, McCave IN (2000) Hydrography and sedimentation under the deep western boundary current on Björn and Gardar Drifts, Iceland Basin. Mar Geol 165:137–169

475 Due L, Van Aken HM, Boldreel LO, Kuijpers A (2006) Seismic and oceanographic evidence
476 of the present-day bottom-water dynamics in the Lousy Bank-Hatton Bank area, NE
477 Atlantic. Deep Sea Res I 53:1729–1741
478 Faugères JC, Mézerais ML, Stow DAV (1993) Contourite drift types and their distribution in
479 the North and South Atlantic Ocean Basins. Sed Geol 82:189–203
480 Faugères JC, Stow DAV, Imbert P, Viana AR (1999) Seismic features diagnostic of
481 contourite drifts. Mar Geol 162:1–38
482 Fernández-Puga MC, Vázquez JT, Somoza L, Díaz-del-Río V, Medialdea T, Mata MP, León
483 R (2007) Gas-related morphologies and diapirism in the Gula of Cádiz. Geo-Mar Lett
484 27:213–221
485 Hammer O, Webb KE, Depreiter D (2009) Numerical simulation of upwelling currents in
486 pockmarks, and data from the Inner Oslofjord, Norway. Geo-Mar Lett 29:269–275
487 Hernández-Molina FJ, Maldonado A, Stow DAV (2008) Abyssal plain contourites. In:
488 Rebesco M, Camerlenghi A (eds) Contourites. Developments in Sedimentology, 60, pp.
489 345–378
490 Hitchen K (2004) The geology of the UK Hatton-Rockall margin. Mar Petrol Geol 21:993–
491 1012
492 Hollister CD, Heezen BC (1972) Geological effects of the ocean bottom currents: Western
493 North Atlantic. In: Gordon AL (eds) Studies in Physical Oceanography. Gordon and
494 Breach, New York, Vol. 2, pp. 37-66
495 Huizhong W, McCave IN (1990) Distinguishing climatic and current effects in mid-
496 Pleistocene sediments of Hatton and Gardar Drifts, NE Atlantic. J Geol Soc Lond
497 147:373–383
498 Hunter S, Wilkinson D, Louarn E, McCave N, Rohling E, Stow DAV, Bacon S (2007) Deep
499 western boundary current dynamics and associated sedimentation on the Eirik Drift,
500 Southern Greenland Margin. Deep Sea Res I 54:2036–2066
501 Johnson H, Ritchie JD, Hitchen K, McInroy DB, Kimbell GS (2005) Aspects of the Cenozoic
502 deformational history of the Northeast Faroe-Shetland Basin, Wyville-Thomson Ridge
503 and Hatton Bank areas. In: Doré AG, Vining BA (eds) Petroleum geology: north-west
504 Europe and global perspectives. Proc of the 6th Petroleum Geology Conf., 6–9 October
505 2003, Geol Soc Lond, pp 993–1007
506 Kimbell GS, Ritchie JD, Johnson H, Gatliff RW (2005) Controls on the structure and
507 evolution of the NE Atlantic margin revealed by regional potential field imaging and 3D
508 modelling. In: Doré AG, Vining BA (eds) Petroleum geology: north-west Europe and

global perspectives. Proc 6th Petroleum Geology Conf., 6–9 October 2003, Geol Soc Lond, pp 933–945

Kuijpers A, Hansen B, Hühnerbach V, Larsen B, Nielsen T, Werner F (2002) Norweian Sea overflow through the Faeroe-Shetland gateway as documented by its bedforms. Mar Geol 188: 147–164

MacLachlan SE, Elliot GM, Parson LM (2008) Investigations of the bottom current sculpted margin of Hatton bank, NE Atlantic. Mar Geol 253:170–184

Masson DG, Wynn RB, Bett BJ (2004) Sedimentary environment of the Faeroe-Shetland Channel and Faeroe Bank channels, NE Atlantic, and the use of bedforms as indicators of bottom current velocity in the deep ocean. Sedimentology 51: 1-35

McCartney MS (1992) Recirculating components to the deep boundary current of the northern North Atlantic. Progr Oceanogr 29:283–383

McCave IN, Tucholke BE (1986) Deep-current controlled sedimentation in the Western North Atlantic. In: Vogt PR, Tucholke BE (eds) The geology of North America, The Western North Atlantic Region, Decade of North American Geology. Geol Soc Am, Boulder, Vol M. pp 451–467

McCave IN, Lonsdale PF, Hollister CD, Gardner WD (1980) Sediment transport over the Hatton and Gardar contourite drifts. J Sed Petrol 50(4):1049–1062

McInroy DM, Hitchen K, Stoker MS (2006) Potencial Eocene and Oligocene stratigraphic traps of the Rockall Plateau, NE Atlantic Margin. In: Allen MR, Goffey GP, Morgan RK, Walker IM (eds). The Deliberate Search for the Stratigraphic Trap. Geol Soc Lond, Special Publications, 254: 247–266

McInroy DM, Hitchen K (2008) Geological evolution and hydrocarbon potential of the Hatton Basin (UK sector), north-east Atlantic Ocean. In: Brown DE (eds) Ext Abstr Vol 38. Central Atlantic Conjugate Margins Conf, 13–15 August 2008, Halifax, Canada. Dalhousie University, Halifax, Nova Scotia. ISBN: 0-9810595-2

Paull CK, Ussler III W, Holbrook WS, Hill TM, Keaten R, Mienert J, Haflidason H, Johnson JE, Winters WJ, Lorenson TD (2008) Origin of pockmarks and chimney structures on the flanks of the Storegga Slide, offshore Norway. Geo-Mar Lett 28:43–51

Roberts D, Bishop DG, Laughton AS, Ziolkowski AM, Scrutton RA, Matthews DH (1970) New sedimentary basin on Rockall Plateau. Nature 225:170–172

Roberts JM, Henry LA, Long D, Hartley JP (2008) Cold-water coral reef frameworks, megafauna communities and evidence for coral carbonate mounds on the Hatton Bank, north east Atlantic. Facies 54:297–316

543 Ruddiman WF (1972) Sediment redistribution on the Reykjanes Ridge: seismic evidence.
544 Geol Soc Am Bull 83:2039–2062
545 Sayago-Gil M, Long D, Fernández-Salas LM, Hitchen K, López-González N, Díaz-del-Río
546 V, Durán-Muñoz P (2009, In Press) Geomorphology of the Talismán Slide (Western
547 slope of Hatton Bank, NE Atlantic Ocean). In: Mosher et al. (eds), Subamrine Mass
548 Movements and Their Consequences, Advances in Natural and Technological Hazards
549 Research, 28:277–288
550 Simpson BA, Ford GD (1999) NW Scotland Offshore Seismicity: Third Annual report to 31
551 March. Br Geol Surv Tech Rep no WL/99/24C
552 Simpson BA, Ford GD, Walker AB (2000) NW Scotland Offshore Seismicity: Fourth Annual
553 report to 31 March. Br Geol Surv Tech Rep no CR/00/24
554 Smith LK, White RS, Kusznir NJ (2005) Structure of the Hatton Basin and adjacent
555 continental margin. In: Doré AG, Vining BS (eds) Petroleum geology: north-west
556 Europe and global perspectives. Proc 6th Petroleum Geology Conf., 6–9 October 2003,
557 Geol Soc Lond, pp 947–956
558 Stoker MS, Akhurst MC, Howe JA, Stow DAV (1998) Sediment drifts and contourites on the
559 continental margin off northwest Britain. Sed Geol 115:33–51
560 Stoker MS, Praeg D, Shannon PM, Hjelstuen BO, Laberg JS, Nielsen T, van Weering TCE,
561 Sejrup HP, Evans D (2005) Neogene evolution of the Atlantic continental margin of
562 NW Europe (Lofoten Islands to SW Ireland): anything but passive. In: Doré AG, Vining
563 BA (eds) Petroleum geology: north-west Europe and global perspectives. Proc of 6th
564 Petroleum Geology Conf, 6–9 October 2003, Geol Soc Lond, pp 1057–1076
565 Stow DAV, Holbrook JA (1984) Hatton Drift contourites, northeast Atlantic, Deep Sea
566 Drilling project LEG 81. In: University of Edinburgh Report no 25, pp 695–699
567 Stow DAV, Hunter S, Wilkinson D, Hernández-Molina FJ (2008) Te nature of contourite
568 deposition. In: Rebesco M, Camerlenghi A (eds) Contourites. Developments in
569 Sedimentology, 60, pp. 143–156
570 Stow DAV, Lovell JPB (1979) Contourites: their recognition in modern and ancient
571 sediments. Earth Sci Rev 14:251–291
572 Tuitt A (2009) Timing and controls of structural inversion in the NE Atlantic Margin.
573 Unpublished PhD thesis. University of Edinburgh, UK
574 Van Aken HM (1995) Mean currents and current variability in the Iceland Basin. J Sea Res
575 33(2):135–145

576 Van Aken HM (2000) The hydrography of the mid-latitude northeast Atlantic Ocean I: the
577 deep water masses. Deep Sea Res I 47:757–788
578 Van Weering TCE, de Haas H, de Stigter HC, Lykke-Andersen H, Kouvaev I (2003)
579 Structure and development of giant carbonate mounds at the SW and SE Rockall
580 Trough margins, NE Atlantic Ocean. Mar Geol 198:67–81
581 Weaver PPE, Wynn RB, Kenyon NH, Evans J (2000) Continental margin sedimentation, with
582 special reference to the north-east Atlantic margin. Sedimentology 47(1):239–256

Captions

Fig. 1 Locality map showing the study area along the north-western margin of the Rockall Plateau, as well as the regional bathymetry and present-day bottom current circulation (*arrows*). *HB* Hatton Bank, *RB* Rockall Bank, *HRB* Hatton-Rockall Basin, *GBB* George Bligh Bank, *FBC* Faeroe Bank Channel, *IB* Iceland Basin. *ISOW* Iceland-Scotland Overflow Water, *AABW* Antarctic Bottom Water, *LDW* Lower Deep Water, *LSW* Labrador Sea Water, *DNBC* Deep Northern Boundary Current (based on McCave et al. 1980; McCartney 1992; Stoker et al. 1998; Bianchi and McCave 2000; Hassold et al. 2006; McLachlan et al. 2008; regional bathymetry from GEBCO-General Bathymetry Chart of the Oceans)

Fig. 2 a Locations of data collection for hill-shade bathymetric imagery and seismic profiling. *Purple lines* Sparker/airgun seismic profiles, *red lines* Topas seismic profiles. **b** Topas seismic section in the southern part of the study area, showing the sedimentary set increasing basinwards, and onlaping upslope as a wedge with well-stratified layers

Fig. 3 a Map showing the two main domains identified in the study area: outcrop and drift. Black line marks the limit between northern (W-E orientation) and southern (SW-NE orientation) part of the bank based on the change of the main trend of the slope. **b** Map showing the variations in slope recorded in the study area, based on multibeam bathymetry data. **c** Large-scale sketch illustrating the main morphologic areas identified on this work. Also indicated are the locations of selected datasets shown in more detail in Fig. 4, 5, 6 and 7

Fig. 4 Selected datasets showing examples of hill-shade bathymetry and vertical depth profiles (location on bathymetry image) used to identify the main morphological features of the study area: **a** moat (arrow indicates moat axis), **b** furrow, **c** scours (arrows indicate scours axis)

Fig. 5 Selected datasets showing examples of hill-shade bathymetry and vertical depth profiles (location on bathymetry image) used to identify the main morphological features of the study area: **a** wave field, **b** contourite-packages boundary (arrow indicates the seabed affected by the limit between two different contourite deposits), **c** ponded deposits (arrows indicating the deposits against ridges)

Fig. 6 Selected datasets showing examples of hill-shade bathymetry and vertical depth profiles (location on bathymetry image) used to identify the main morphological features of the study area: **a** scarps (arrows indicate the gradient changes), **b** gullies, **c** ridges (arrows indicate barriers axis with mounds on top), **d** depressions (arrows indicate hollows)

Fig. 7 Hill-shade bathymetry, 3D image and topas seismic section (location on bathymetry image) of the Talismán Slide identified in southern part of the study area

Fig. 8 a Large-scale sketch presented in figure 3 illustrating the seabed morphologic details in the northern (**b**) and southern (**c**, **d**) parts of the Hatton Bank. Morphological features of the main areas describe in this work can be observed in detail in **b**, **c**, **d.** The outcrop area (**a**) is characterized by an uneven surface with crest and scarps (**b**, **c**, **d**) and the ridges area can be seen with ponded deposits associated (**b**). The smooth surface (**a**) is nearly a flat surface located in the southern part of the bank (**b**, **c**, **d**). Bedforms area (**a**) are describe as a surface with different morphologies as furrows, scours and scarps (**b**, **c**, **d**) located in the northern part as well as in the southern part of the bank. Slides (**a**) can be seen in the southern part (**c**, **d**) close to bedforms areas. The slide located in **d** is the Talismán Slide describe in this work.

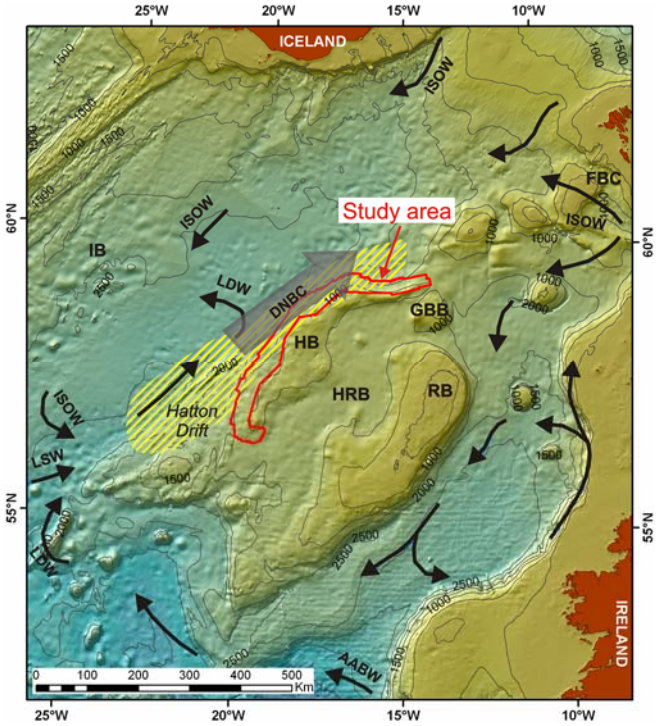
25°W
20°W
15°W
10°W
60°N
55°N
ICELAND
IRELAND
Study area
ISOW
FBC
IB
LDW
DNBC
GBB
HB
HRB
RB
Hatton
Drift
LSW
AABW
0 100 200 300 400 500 Km

Fig.1

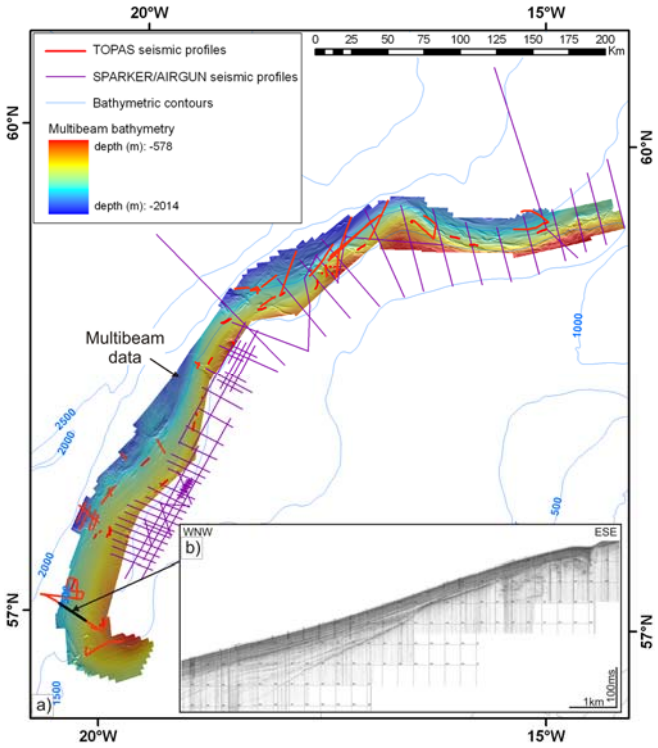
20°W
15°W
60°N
57°N
TOPAS seismic profiles
SPARKER/AIRGUN seismic profiles
Bathymetric contours
Multibeam bathymetry
depth (m): -578
depth (m): -2014
0 25 50 75 100 125 150 175 200 Km
Multibeam
data
WNW
ESE
b)
a)
1km
100ms

Fig.2

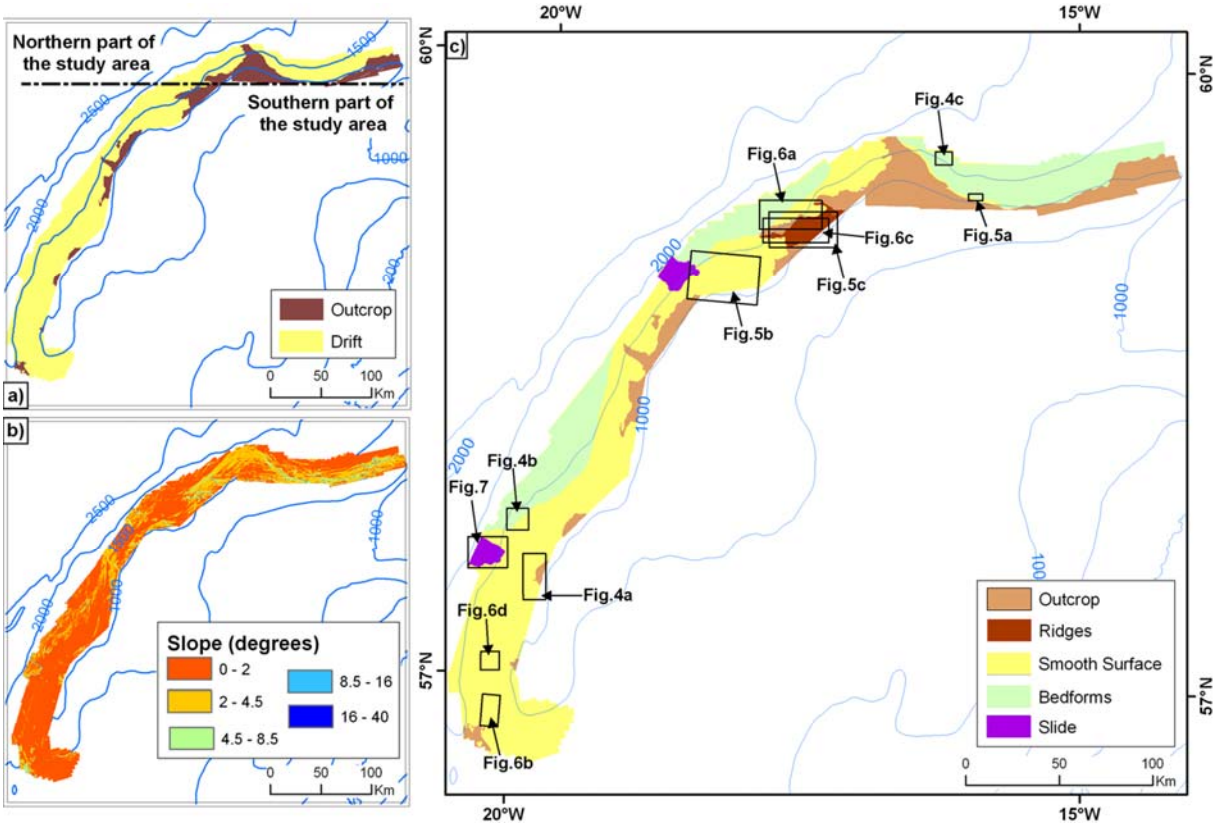
Northern part of the study area
Southern part of the study area
Outcrop
Drift
0 50 100 Km
a)
b)
Slope (degrees)
0 - 2
2 - 4.5
4.5 - 8.5
8.5 - 16
16 - 40
0 50 100 Km
c)
20°W
15°W
60°N
57°N
Fig.4c
Fig.6a
Fig.6c
Fig.5a
Fig.5c
Fig.5b
Fig.4b
Fig.7
Fig.4a
Fig.6d
Fig.6b
Outcrop
Ridges
Smooth Surface
Bedforms
Slide
0 50 100 Km

Fig.3

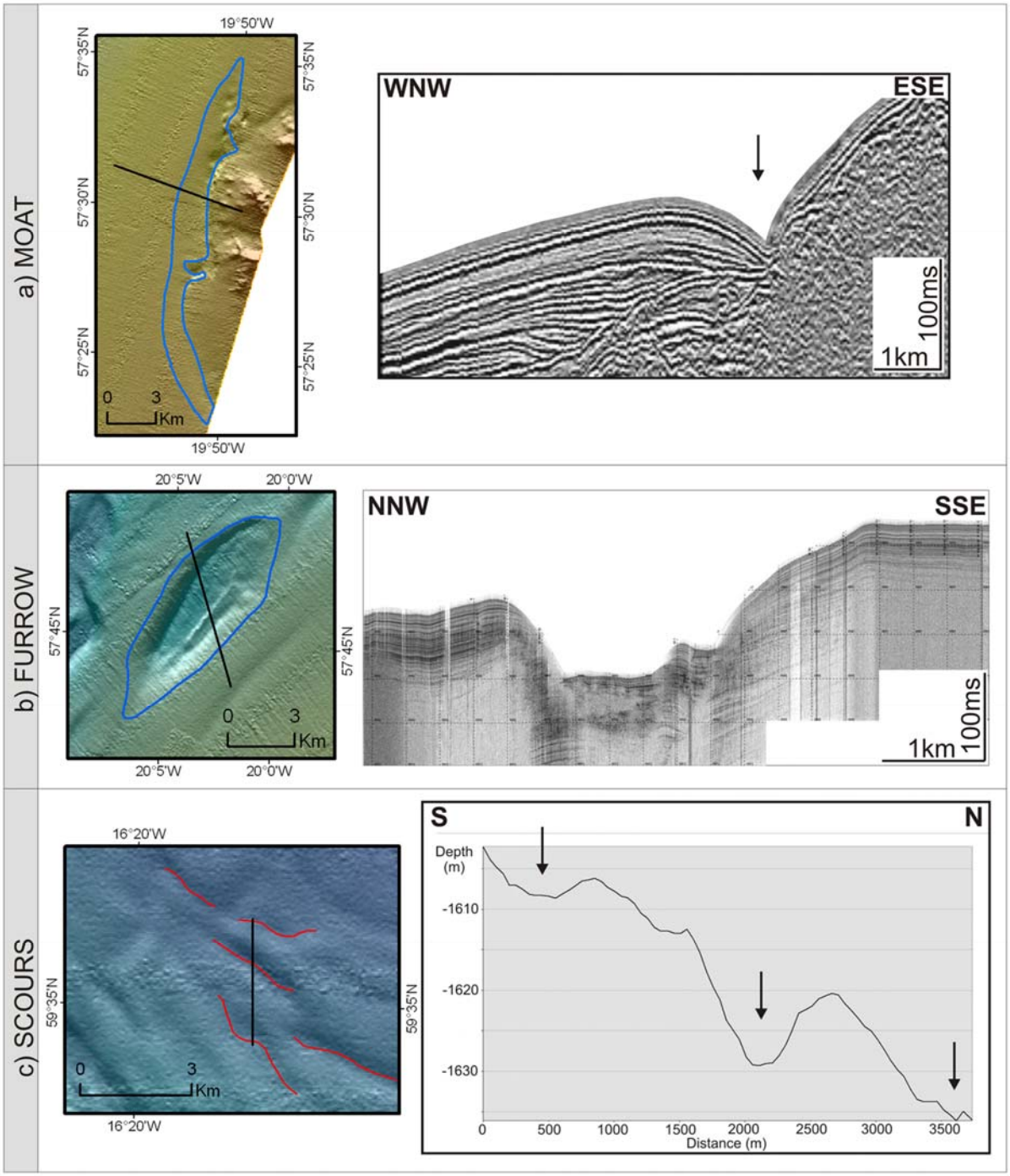
a) MOAT
19°50'W
57°35'N
57°30'N
57°25'N
0
3
Km
WNW
ESE
100ms
1km
b) FURROW
20°5'W
20°0'W
57°45'N
NNW
SSE
c) SCOURS
16°20'W
59°35'N
S
N
Depth (m)
-1610
-1620
-1630
0
500
1000
1500
2000
2500
3000
3500
Distance (m)

Fig.4

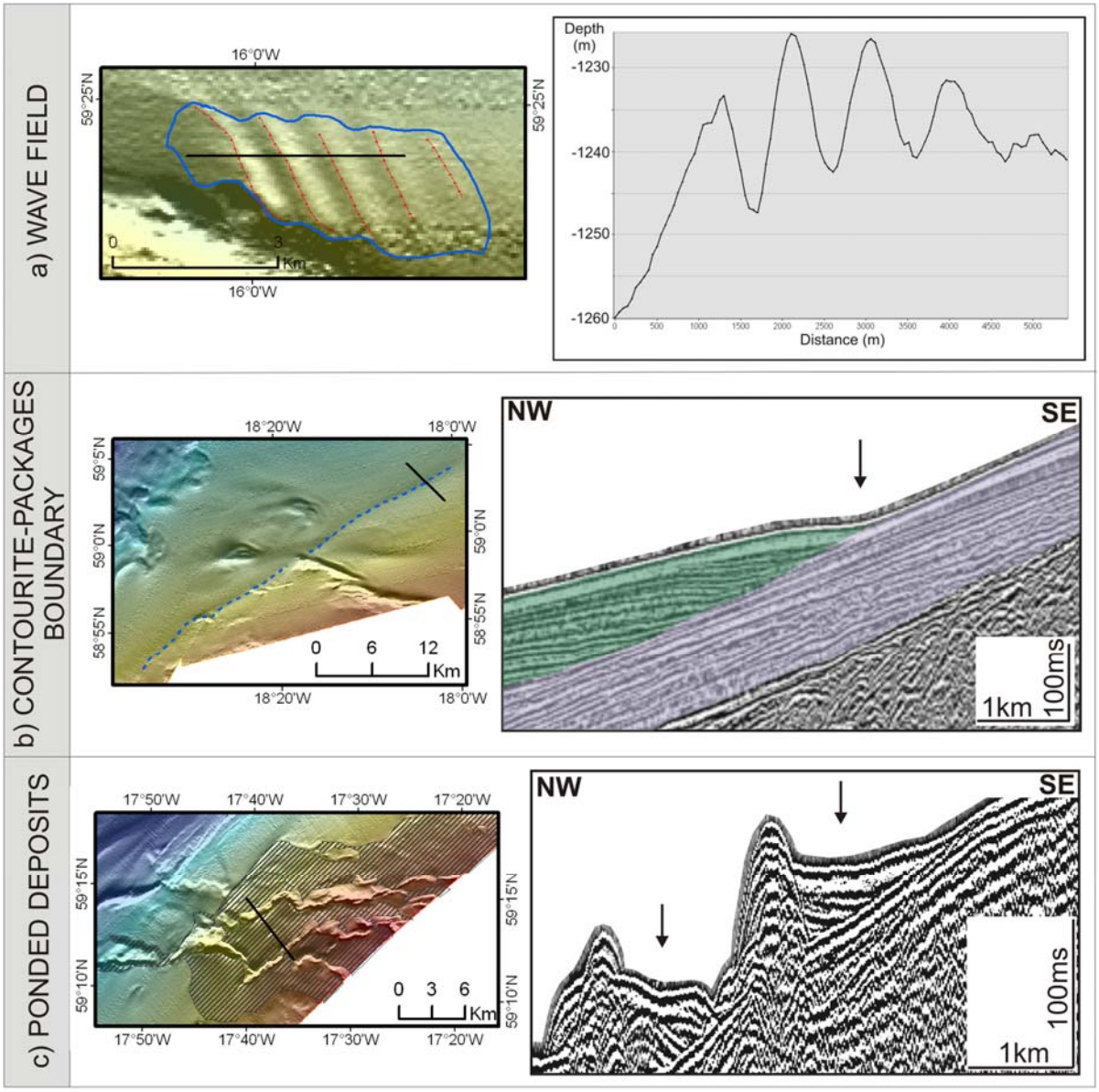
a) WAVE FIELD
16°0'W
59°25'N
0
3
Km
16°0'W
59°25'N
Depth
(m)
-1230
-1240
-1250
-1260
0
500
1000
1500
2000
2500
3000
3500
4000
4500
5000
Distance (m)
b) CONTOURITE-PACKAGES BOUNDARY
18°20'W
18°0'W
59°5'N
59°0'N
58°55'N
0
6
12
Km
18°20'W
18°0'W
59°0'N
58°55'N
NW
SE
1km
100ms
c) PONDED DEPOSITS
17°50'W
17°40'W
17°30'W
17°20'W
59°15'N
59°10'N
0
3
6
Km
17°50'W
17°40'W
17°30'W
17°20'W
59°15'N
59°10'N
NW
SE
100ms
1km

Fig.5

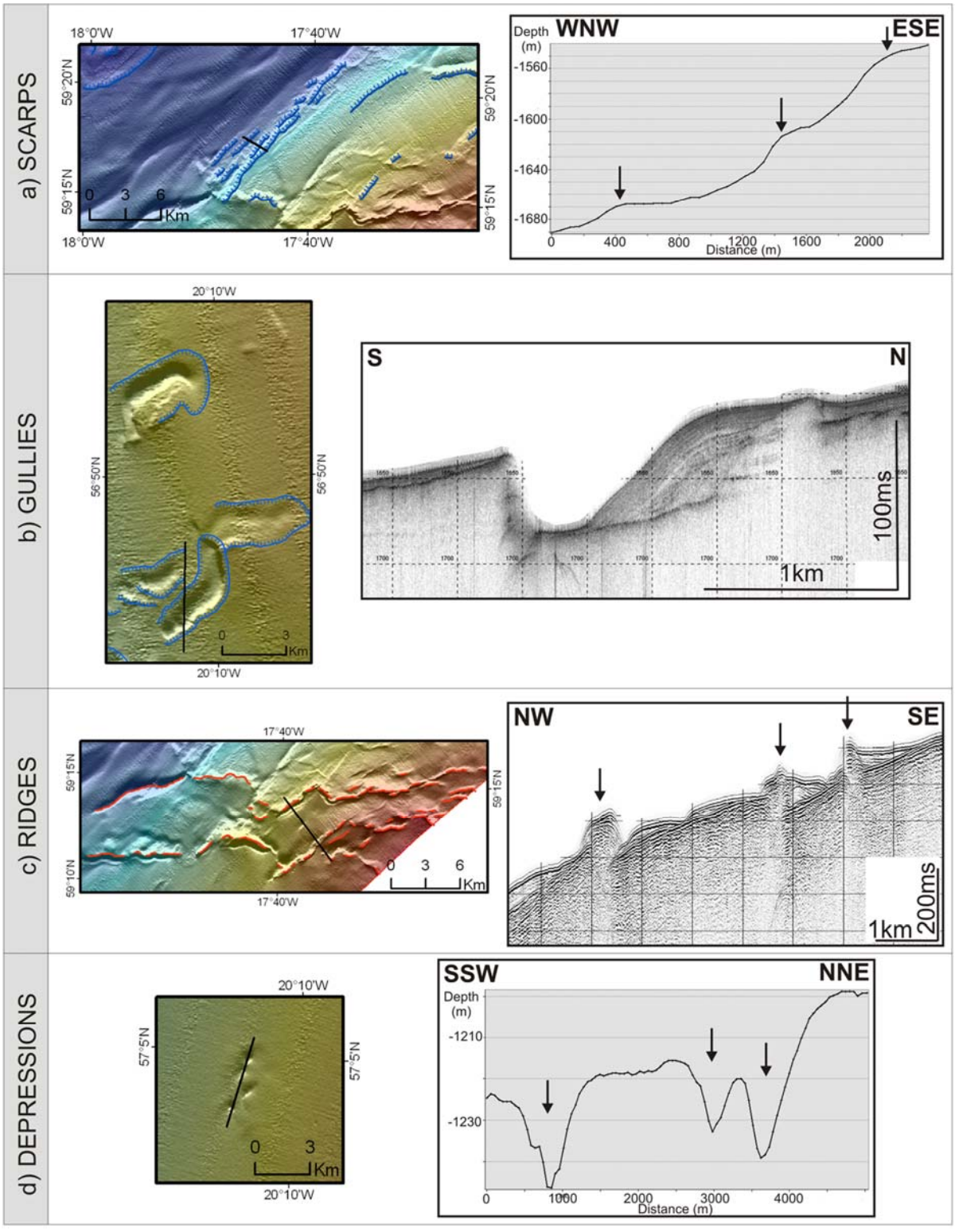
a) SCARPS
18°0'W
17°40'W
59°20'N
59°15'N
0 3 6 Km
Depth (m)
WNW
ESE
-1560
-1600
-1640
-1680
0 400 800 1200 1600 2000
Distance (m)
b) GULLIES
20°10'W
56°50'N
0 3 Km
S
N
100ms
1km
c) RIDGES
17°40'W
59°15'N
59°10'N
0 3 6 Km
NW
SE
200ms
1km
d) DEPRESSIONS
20°10'W
57°5'N
0 3 Km
SSW
NNE
Depth (m)
-1210
-1230
0 1000 2000 3000 4000
Distance (m)

Fig.6

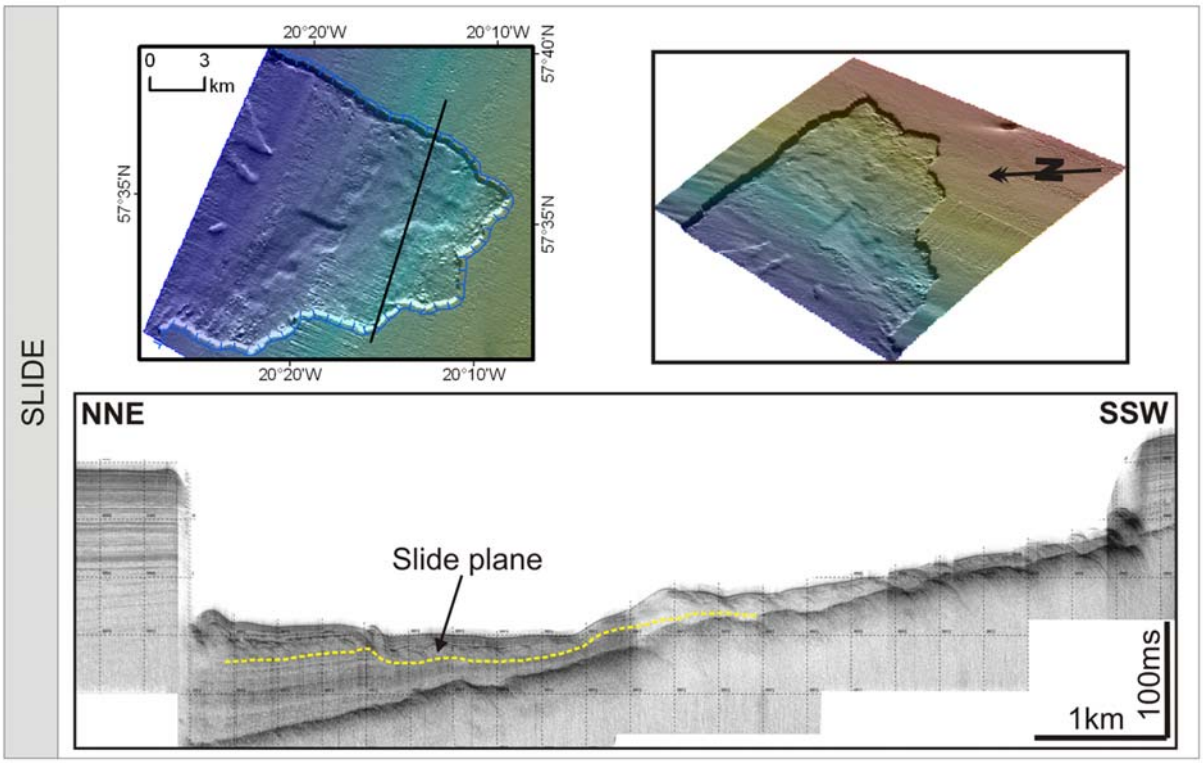
SLIDE
20°20'W
20°10'W
57°40'N
57°35'N
0 3
km
N
NNE
SSW
Slide plane
1km
100ms

Fig.7

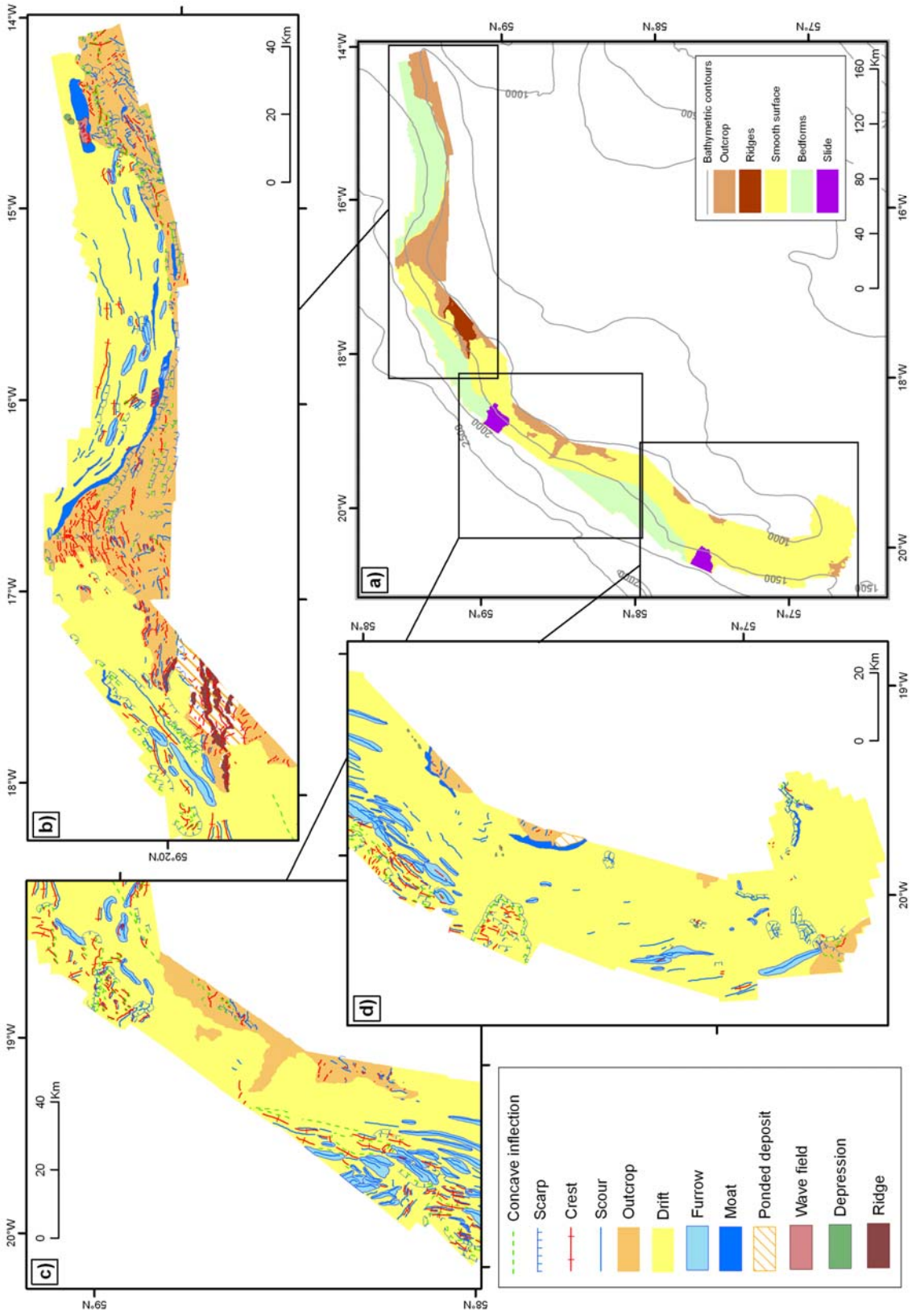
a)
b)
c)
d)
Bathymetric contours
Outcrop
Ridges
Smooth surface
Bedforms
Slide
Concave inflection
Scarp
Crest
Scour
Outcrop
Drift
Furrow
Moat
Ponded deposit
Wave field
Depression
Ridge
Km

Fig.8